High-energy trapped protons measured by PAMELA

Alessandro Bruno

NASA/GSFC

on behalf of the PAMELA collaboration

IRENE Space Radiation Modelling and Data Analysis Workshop 2019

29-31 May 2019, Sykia, Greece

The PAMELA collaboration

Payload for Antimatter Matter Exploration and Light-nuclei Astrophysics

Italy: Bari, Florence, Frascati, Naples, Rome, Trieste, CNR, Florence

Russia: Moscow, St. Petersburg

Ioffe Physico-Technical Institute

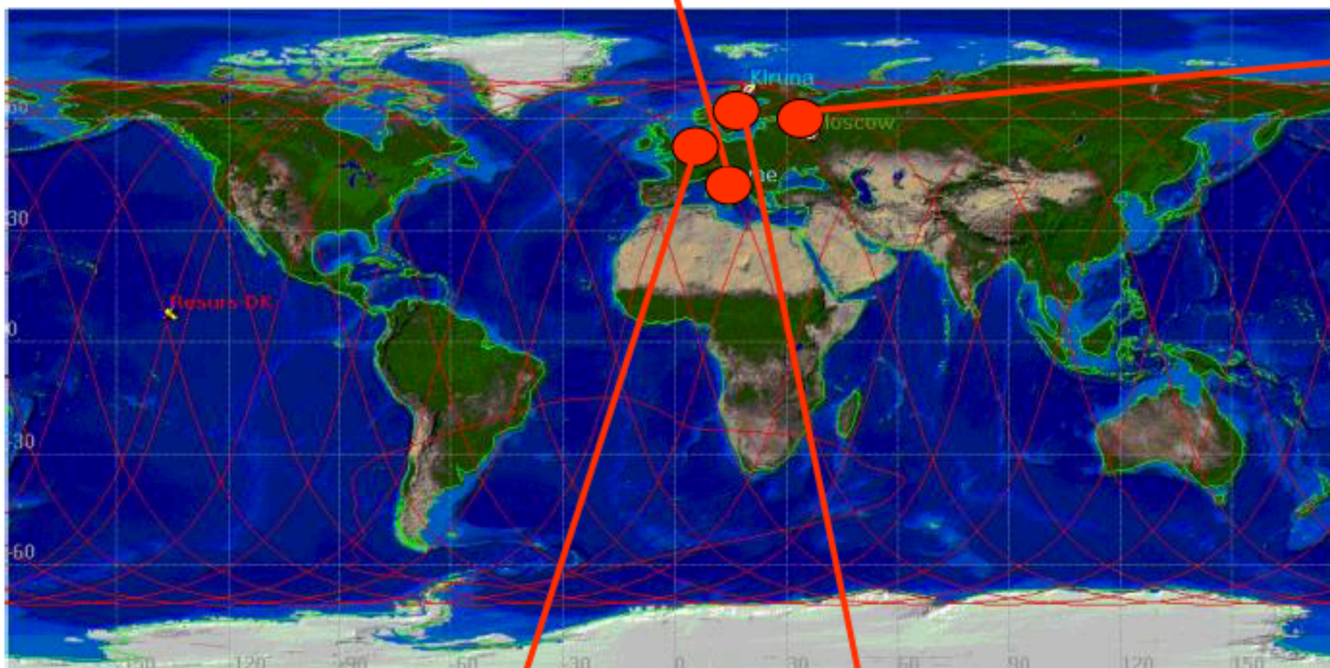

Germany: Siegen

Universität Gesamthochschule Siegen

Sweden: KTH, Stockholm

Kungl Tekniska Högskolan

PAMELA scientific goals



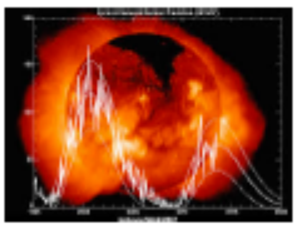
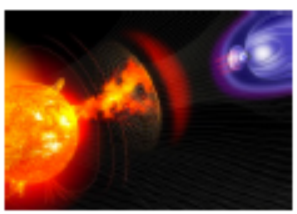
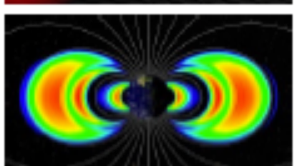

- **Precise measurements of protons, electrons, their antiparticles and light nuclei in the cosmic radiation**
- Research for Dark Matter indirect signatures
- Exploration of the particle/antiparticle symmetry
- Investigation of the CR origin and propagation mechanisms in the Galaxy, the heliosphere and the terrestrial magnetosphere
- Detailed measurement of the high energy particle populations (galactic, solar, **geomagnetically trapped** and albedo) in the near-Earth radiation environment

The PAMELA experiment

Main requirements → high-sensitivity particle identification and precise momentum measure

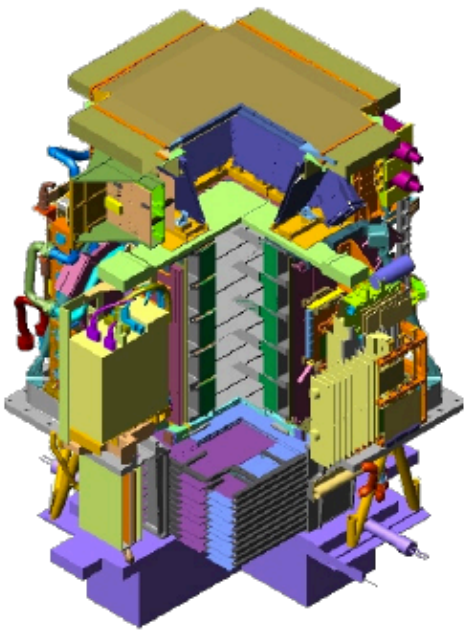

Size: 130x70x70 cm^3
GF: 21.5 cm^2 sr
Mass: 470 kg
Power Budget: 360W

Resurs DK-1 satellite:
Semi-polar (70° inclination) and elliptical (350÷610 km altitude) orbit

Time-Of-Flight
plastic scintillators + PMT
- Trigger
- Albedo rejection;
- Mass identification up to 1 GeV;
- Charge identification from dE/dX.

Anticoincidence shield
plastic scintillators + PMT

Electromagnetic calorimeter
W/Si sampling (16.3 X_0, 0.6 λI)
- Discrimination e+ / p, anti-p / e^- (shower topology)
- Direct E measurement for e^-

Bottom scintillator (+PMT)

Neutron detector
^{3}He counters
- High-energy e/h discrimination

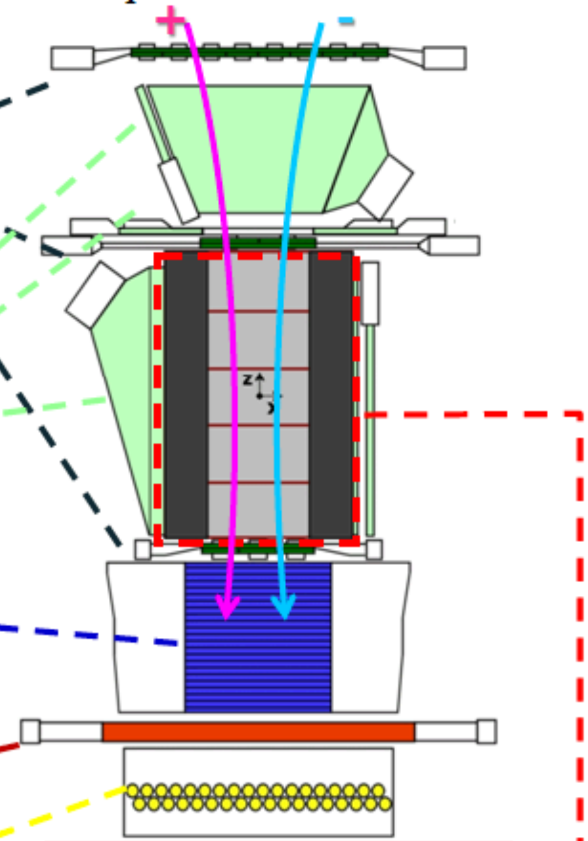

Spectrometer
microstrip silicon tracking system + permanent magnet
- Magnetic rigidity: R=pc/Ze
- Charge sign
- Charge value from dE/dx
- Particle direction

The PAMELA experiment

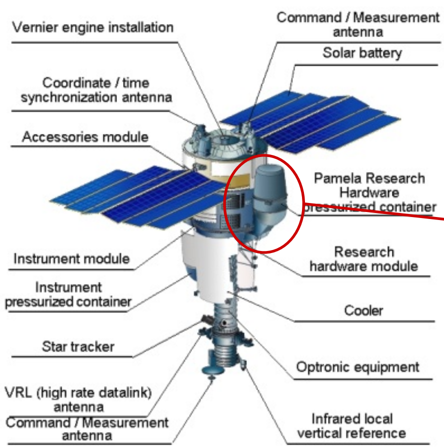

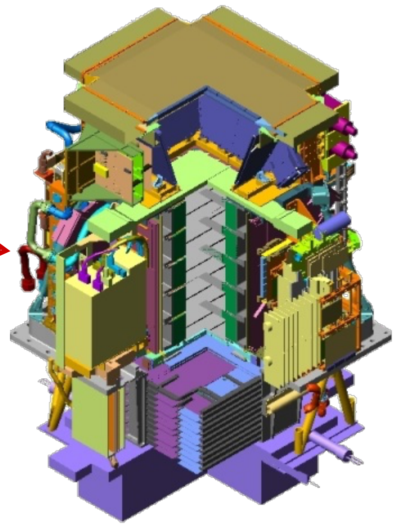

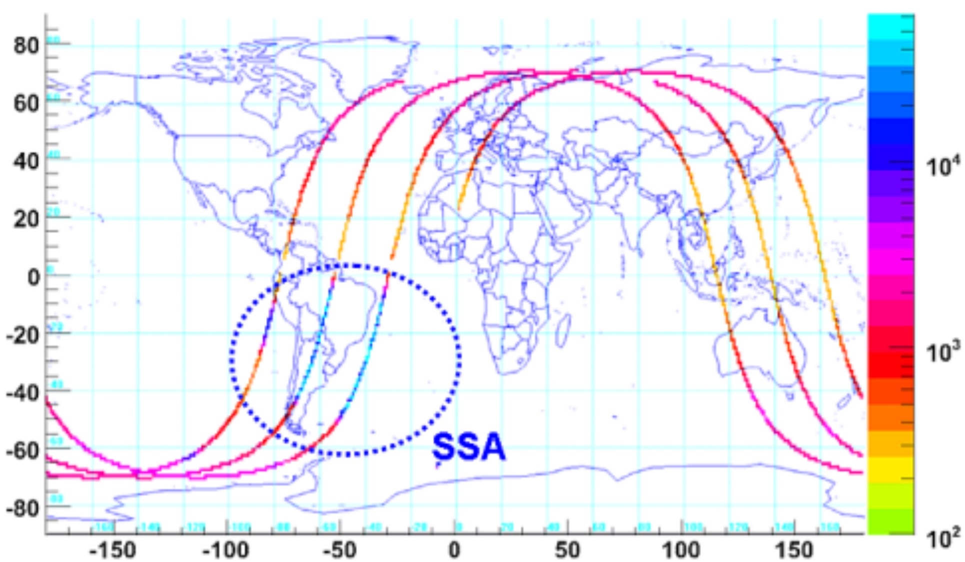

- **precise rigidity measurements**
  - wide range (400 MV — 1.2 TV)
- **sensitive to composition**
  - p/pbar, e+/e-, light nuclei
- **semi-polar (70 deg) and elliptic (350 - 610 km) orbit**
  - low energy CRs & SEPs (polar caps)
  - geomagnetically trapped (SAA) and albedo
  - changed to approx. circular orbit (~580 km) in 2010
- **good angular resolution (~2 deg)**
  - possibility to investigate flux angular distributions (anisotropies)
- **PAMELA took data up until the loss of contact in 2016 Jan**
  - Almost 10 years of data taking!!!

PAMELA's measurements of under-cutoff cosmic-rays

- **Measurements of quasi-trapped electron and positron fluxes with PAMELA**, Adriani *et al* 2009, J. Geophys. Res., Volume 114, Issue A12, DOI: 10.1029/2009JA014660

- **The discovery of geomagnetically trapped cosmic-ray antiprotons**, Adriani *et al* 2011, *ApJL* 737 L29, DOI: 10.1088/2041-8205/737/2/L29

- **Trapped proton fluxes at low Earth orbits measured by the PAMELA experiment**, Adriani *et al* 2015, *ApJL* 799 L4, DOI: 10.1088/2041-8205/799/1/L4

- **Reentrant albedo proton fluxes measured by the PAMELA experiment**, Adriani *et al* 2015, J. Geophys. Res. Space Phys. 120, no.5, 3728-3738, DOI: 10.1002/2015JA021019

- **PAMELA's measurements of geomagnetic cutoff variations during the 14 December 2006 storm**, Adriani *et al* 2016, Space Weather, Volume 14, Issue 3, pp. 210-220, DOI: 10.1002/2016SW001364

- **Trapped positrons observed by PAMELA experiment**, Mikhailov *et al* 2016, J. Phys.: Conf. Ser. 675 032003, DOI: 10.1088/1742-6596/675/3/032003

Adiabatic invariants

Data analyzed in the frame of **adiabatic theory** of particle motion in the geomagnetic field

Gyro motion:

- V x B acceleration leads to gyro motion about field lines
- frequencies ~kHz
- associated 1st invariant μ, relativistic magnetic moment:

$$\mu = \frac{p^2 \sin^2 \alpha}{2 m_0 B}$$

pitch angle α: $\tan \alpha = \frac{V_\perp}{V_\parallel}$

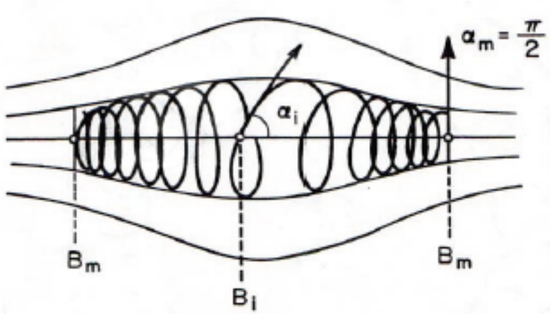

Bounce motion:

- As a particle gyrates down field line, the pitch angle increases as B increases
- Motion along field line reverses when pitch angle reaches 90° (mirror point)
- period ~sec
- associated 2nd invariant K longitudinal invariant:

$$K = \int_{-l_m}^{+l_m} p_\parallel \, dl$$

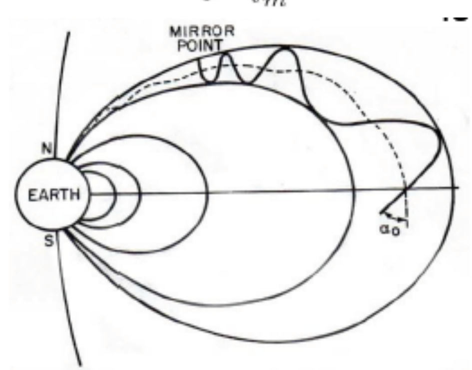

Drift motion:

- Gradient in magnetic field leads to drift motion around Earth: east for electrons, west for protons/ions
- period ~minutes
- associated 3rd invariant ϕ, magnetic flux:

$$\Phi = -\frac{2\pi B_E R_E^2}{L}$$

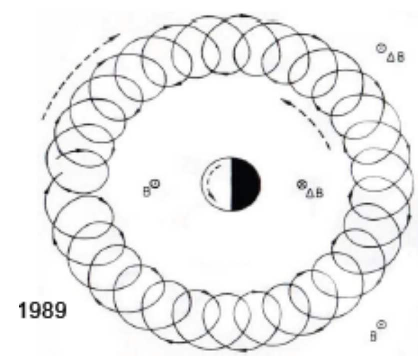

Particle classification

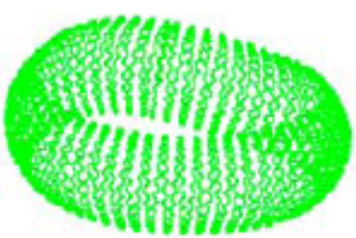

- **stably-trapped** protons perform several drift cycles (>4) around the Earth without intercepting the absorbing atmosphere limit.
  - They satisfy adiabatic conditions: $\omega_{bounce}/\omega_{gyro} \leq 0.3$ and $\omega_{drift}/\omega_{bounce} \leq 0.01$
  - NB: the tracing technique allowed to account for the breakdown of trapping at high energies

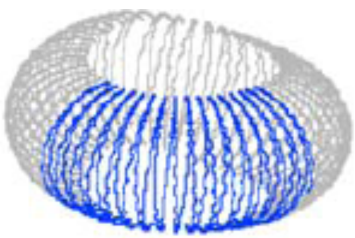

- **Re-entrant albedo** protons can be classified into:
  - **quasi-trapped** protons:
    - trajectories similar to those of stably-trapped protons, but are originated and re-absorbed by the atmosphere during a time larger than a bounce period

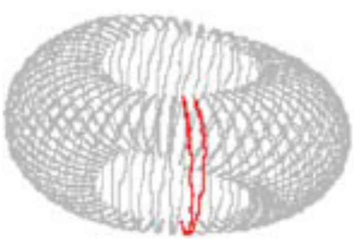

  - **precipitating** protons (untrapped):
    - originated and re-absorbed by the atmosphere within a bounce period.
  - **pseudo-trapped** protons (penumbra):
    - Non-adiabatic or large gyro-radius effects cause the breakdown of trapping conditions
      - irregular trajectories with no periodicity
      - large distances from the detection location

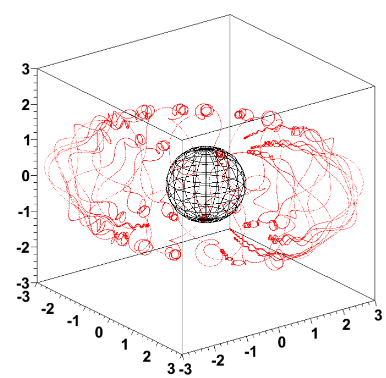

Flux evaluation

Flux anisotropy and detector effective area

- The factor of proportionality between particle fluxes and count-rates is given by the detector gathering power (Sullivan 1971):

$$\Gamma_F = \int_\Omega d\omega F(\omega) \int_S d\sigma \cdot \hat{r} = \int_\Omega d\omega F(\omega) A(\omega)$$

- For isotropic particles, $F(\omega)=1$, and Γ_F is independent on particle directions.

- However, particle fluxes in the SAA are **highly anisotropic** because of the interaction with the atmosphere ($0<F(\omega)<1$)
- We defined an affective area as a function of the spacecraft orientation **Ψ** wrt local **B**, local pitch-angle **α** and energy **E** (averaged over gyro-phase angle **β**)

$$H(\Psi,\alpha,E) = \frac{1}{2\pi} \int_0^{2\pi} d\beta \left[A\big(E, \vartheta(\Psi,\alpha,\beta), \varphi(\Psi,\alpha,\beta)\big) \cos\vartheta(\Psi,\alpha,\beta) \sin\alpha \right]$$

  where $\vartheta = \vartheta(\alpha,\beta), \varphi = \varphi(\alpha,\beta)$ describe the particle direction in the detector frame.
- The relationship between local and geomagnetic angles depends on the spacecraft orientation

Flux evaluation

Flux anisotropy and detector effective area

- To reduce statistical fluctuations in each (E_k,α,Ψ) bin, a **mean effective area** was derived at each spacecraft location X=(lat,lon,alt):

$$H(\mathbf{X}, E_k, \alpha) = \frac{\sum_{\Psi \to \mathbf{X}} H(E_k, \alpha, \Psi) \cdot T(\Psi)}{\sum_{\Psi \to \mathbf{X}} T(\Psi)}$$

  by weighting each area contribution by the livetime spent at spacecraft orientations corresponding to X.

- Differential directional fluxes were calculated over a **5-D grid**:

$$F(\mathbf{X}, E_k, \alpha) = \frac{N(\mathbf{X}, E_k, \alpha)}{2\pi \cdot H(\mathbf{X}, E_k, \alpha) \cdot T(\mathbf{X}) \cdot \Delta\alpha \cdot \Delta E_k}$$

  where N(X,E_k,α) is the number of counts corrected by selection efficiencies and T(X) is the livetime spent at X.

- Grid resolution: 2 deg for latitude & longitude; 20 km for altitude
- Data recorded by PAMELA between **July 2006 and Sept. 2009**
- Time variations studied over 5 bunches of data, each of ~**244 days** (satellite precession)

Flux calculation

$F(\mathbf{X},\alpha,E)$

geographic grid

$\mathbf{X}$=(Lat,Lon,Alt)

East-West effect

$F(\mathbf{X}_{GC},\alpha,E)$

guiding center correction

interpolation

$F(\mathbf{K},\Phi,E)$

invariant coordinates

1) adiabatic invariants
2) Roeder/McIlwain L-shell vs eq. pitch angle
3) invariant altitude vs magnetic latitude

Geographic Maps

columns: same energy bins
rows: same altitude bins

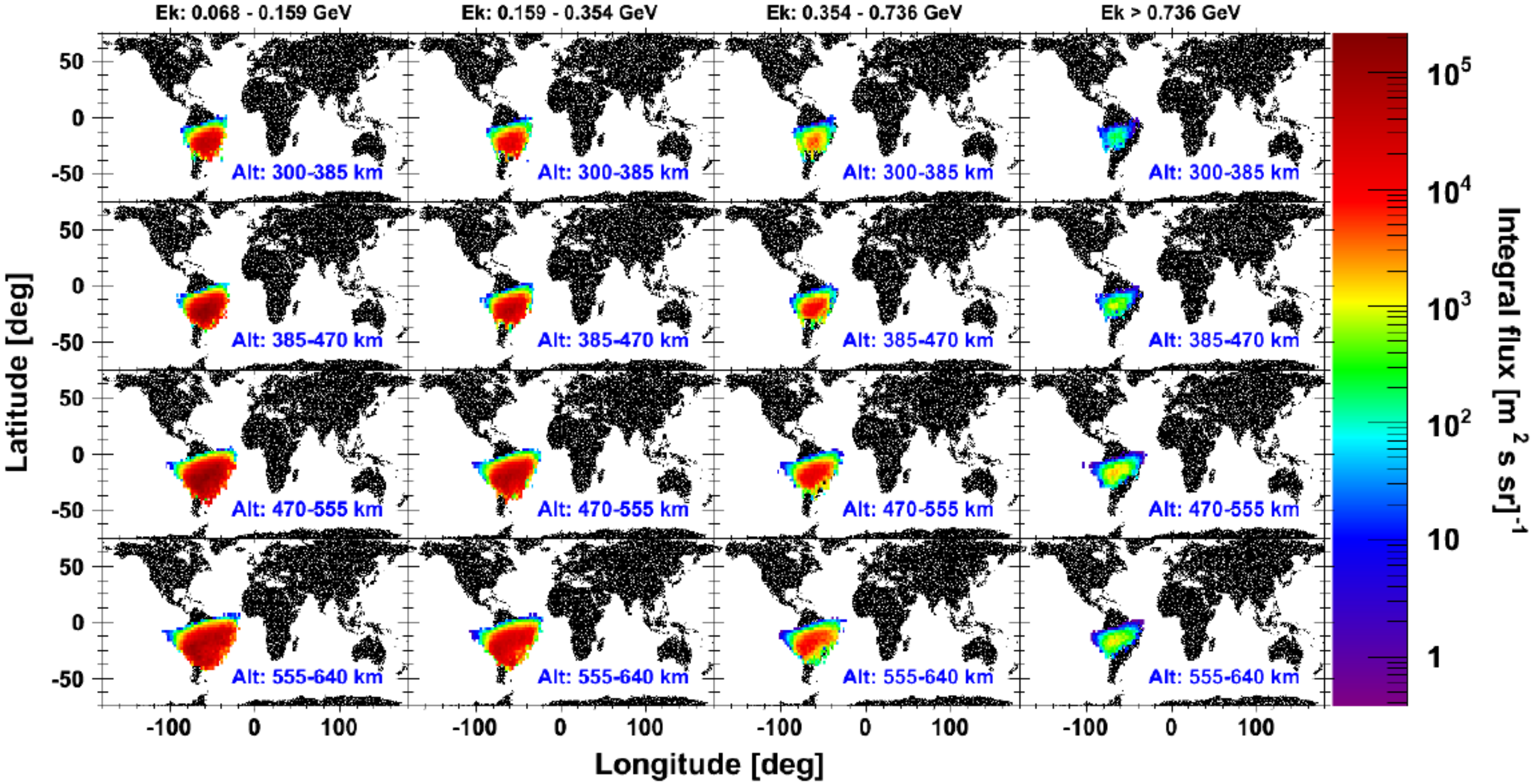

Stably-trapped integral flux ($m^{-2}s^{-1}sr^{-1}$) averaged over the pitch angle range covered by PAMELA, as a function of geographic coordinates, evaluated for different energy (columns) and guiding center altitude (rows) bins.

Fluxes vs adiabatic invariants

$$K = \int_{s_m}^{s'_m} [B_m - B(s)]^{1/2} ds$$

$$\Phi = \oint \mathbf{A} \cdot \mathbf{dl}$$

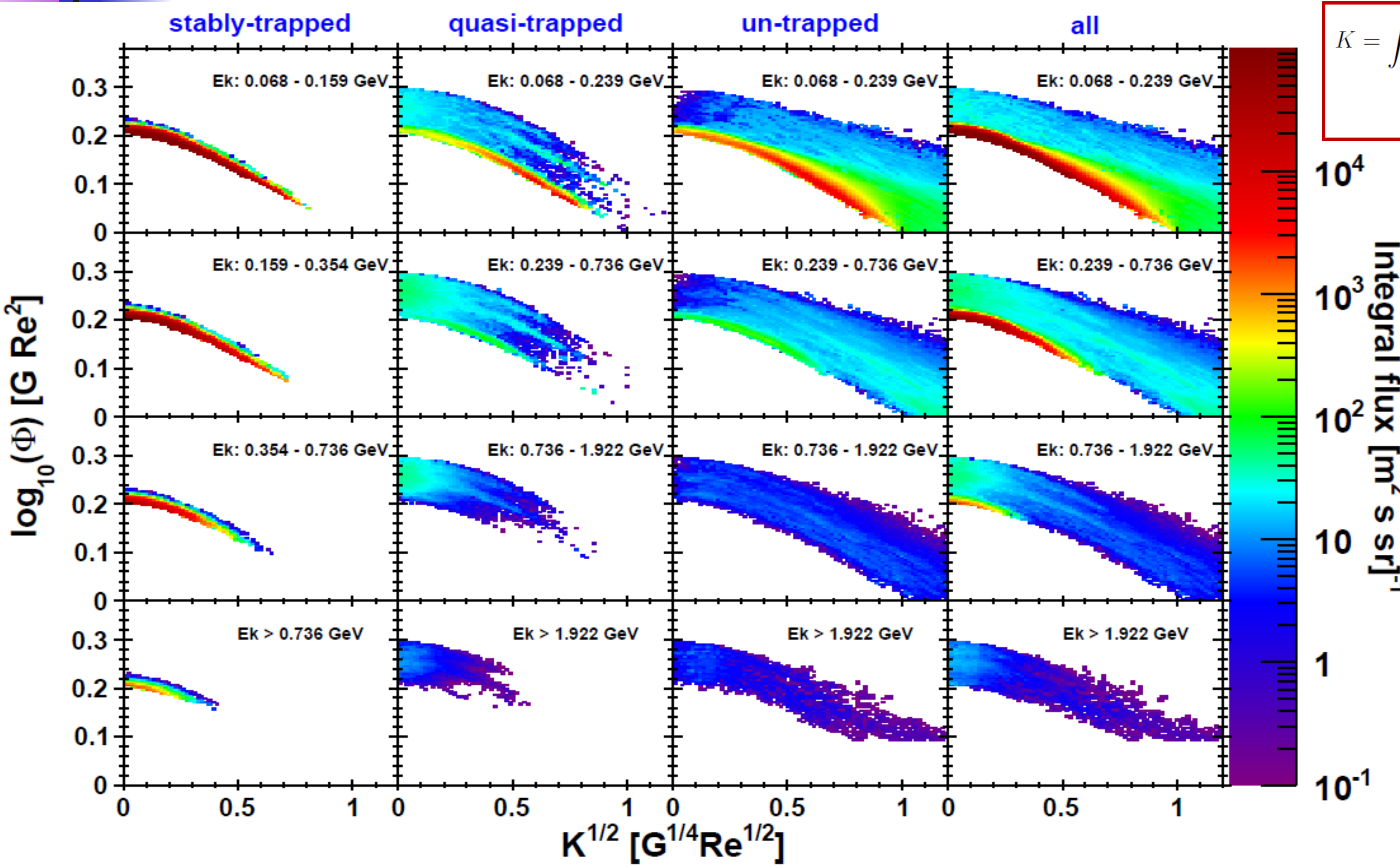

Proton integral fluxes ($m^{-2}s^{-1}sr^{-1}$) as a function of the second K and the third Φ adiabatic invariant, for different kinetic energy bins (see the labels).

Results for the different populations are reported (from left to right): stably-trapped, quasi-trapped, un-trapped and the total under-cutoff proton sample.

Fluxes vs L & eq. pitch angle

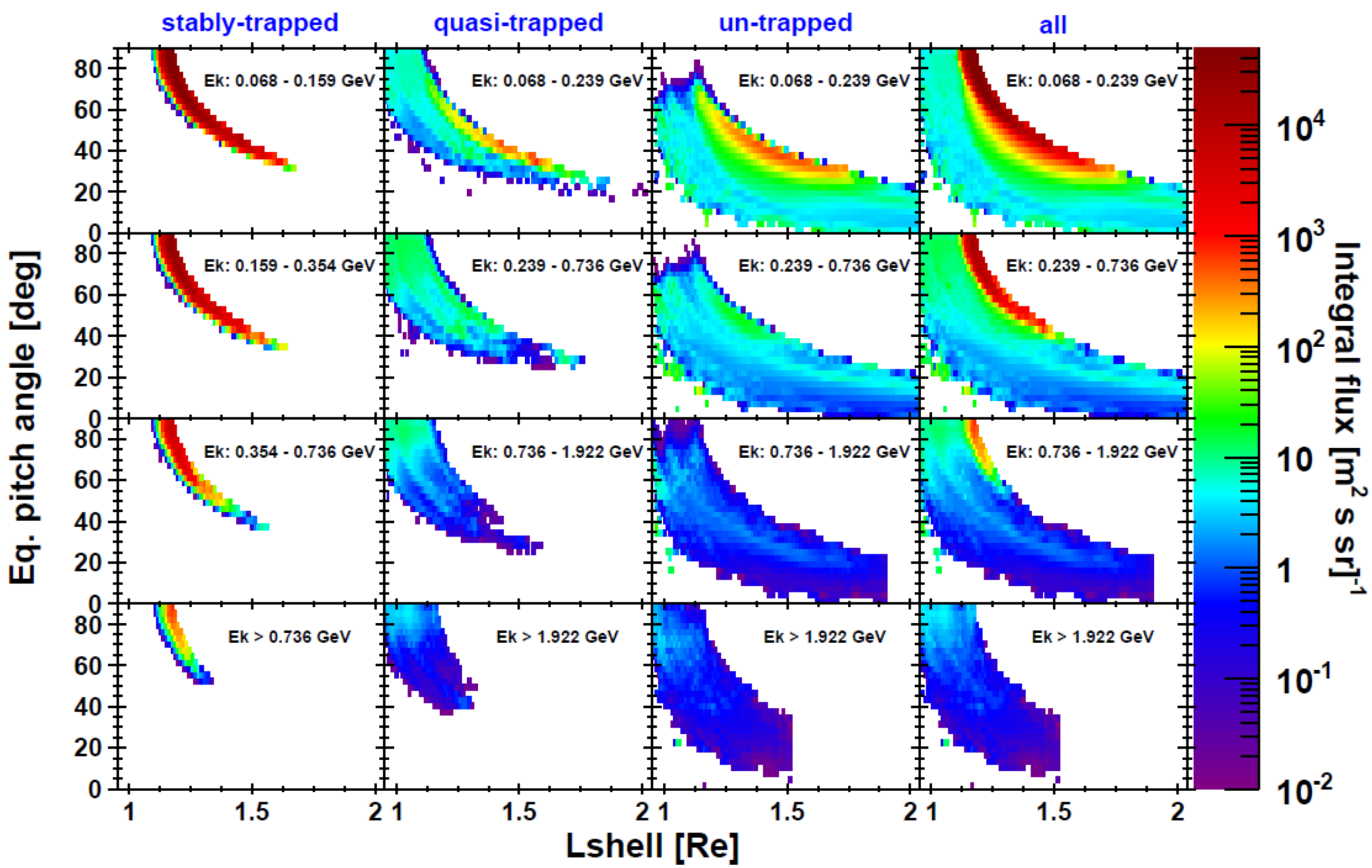

Proton integral fluxes ($m^{-2}s^{-1}sr^{-1}$) as a function of equatorial pitch angle and McIlwain's L-shell, for different kinetic energy bins (see the labels).
Results for the different populations are reported (from left to right): stably-trapped, quasi-trapped, un-trapped and the total under-cutoff proton sample.

Comparison with semi-emphirical models

Stably-trapped differential fluxes ($GeV^{-1}m^{-2}s^{-1}sr^{-1}$) compared with predictions from **AP8-min** (Sawyer & Vette 1976) and **PSB97** (Heynderickx et al. 1999) semi-empirical models, denoted with dashed black line and the solid blue line respectively. Model calculations from the SPENVIS on-line system (Heynderickx et al. 2000).

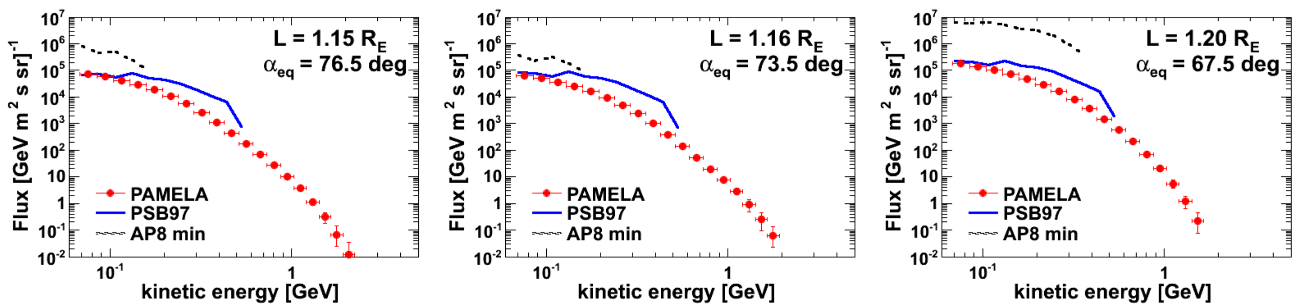

sample energy spectra for three combinations of equatorial pitch angle and McIlwain's L-shell

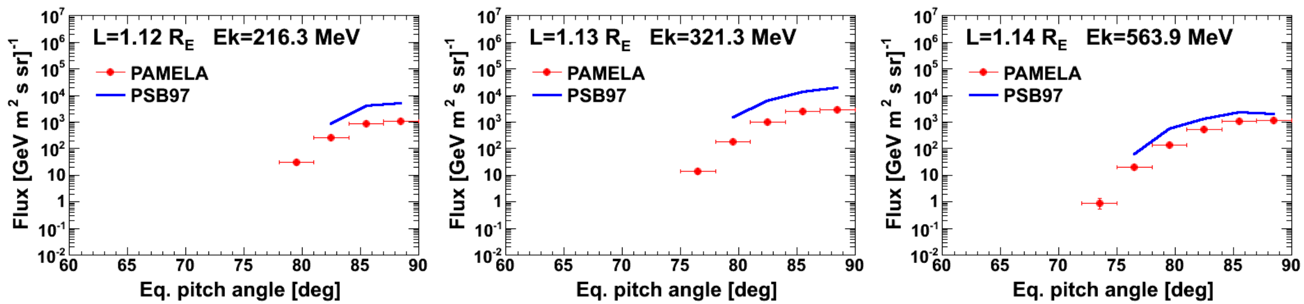

equatorial pitch angle profiles for three combinations of kinetic energy and L-shell values

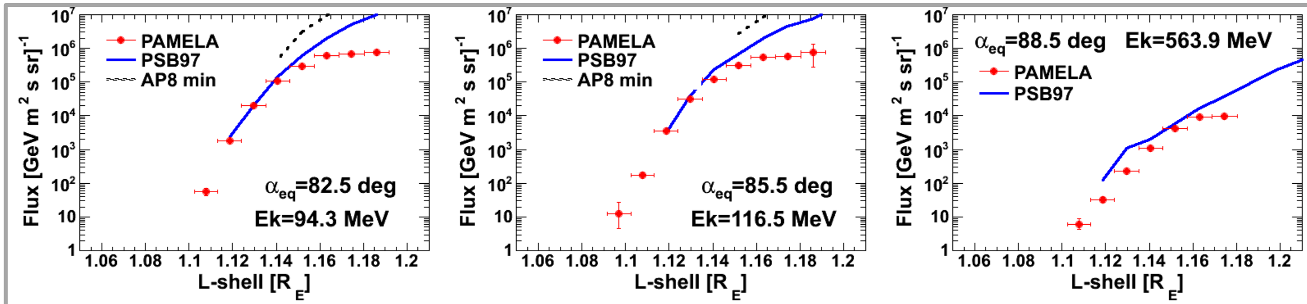

L-shell profiles for three combinations of kinetic energies and equatorial pitch angles.

Comparison with Selesnick model

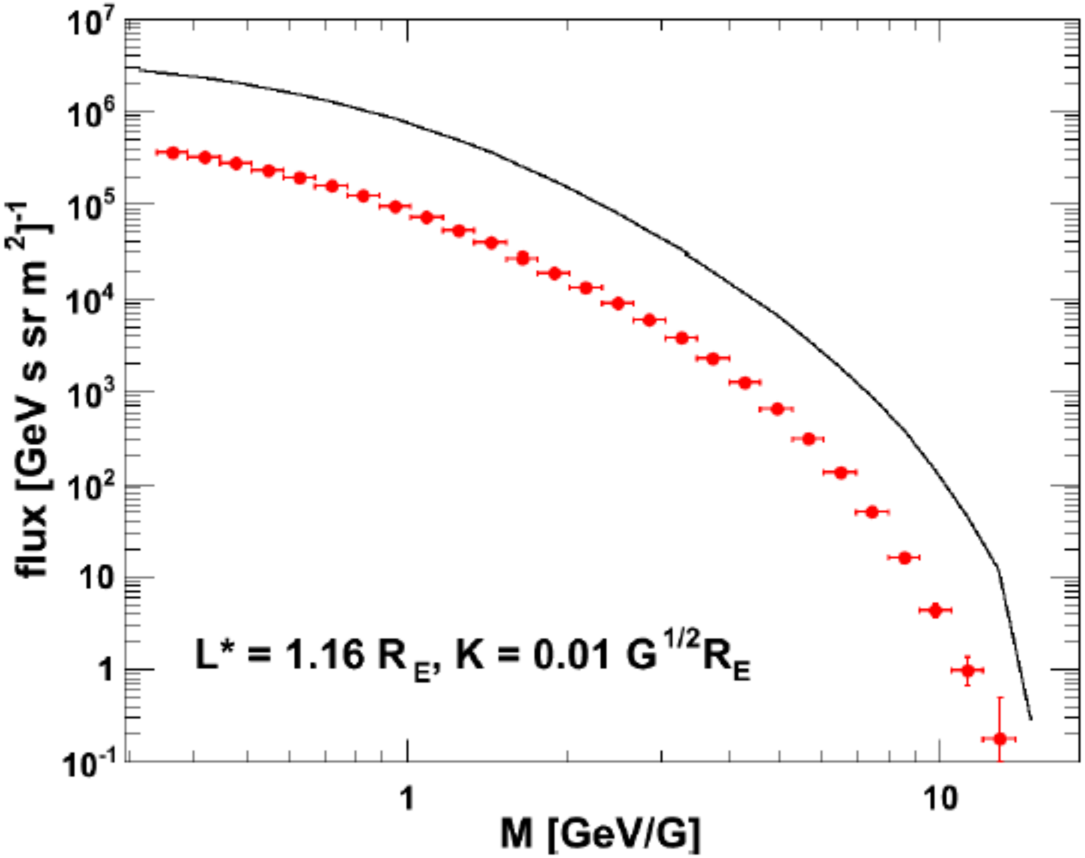

$$L^* = \frac{2\pi\mu_E}{R_E\Phi}$$

Stably-trapped differential flux ($GeV^{-1}m^{-2}s^{-1}sr^{-1}$) at geomagnetic equator compared with a theoretical calculation by Selesnick et al. (2007) for the year 2000. Spectra are reported as a function of first adiabatic invariant M, for sample values of K (second adiabatic invariant) and L* (Roeder parameter) invariants.

Conclusions

- PAMELA data improve the description of **high-energy** trapped protons at **low altitudes (SAA)**

- The analyzed data set will be extended with the inclusion of data acquired after September 2009

- We will work with the AP9/IRENE team to implement the PAMELA data in the model
  - 5-dim grid (*lat, lon, alt,* α*,* E_k) of trapped fluxes
  - Time variations (2006-2015) studied over *n* intervals (e.g. based on spacecraft orbit precession)

Backup slides

Albedo classification

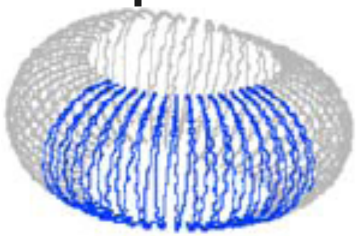

Lifetime = the time between the particle origin (traced backward) and its subsequent absorption (traced forward) in the atmosphere (40 km).

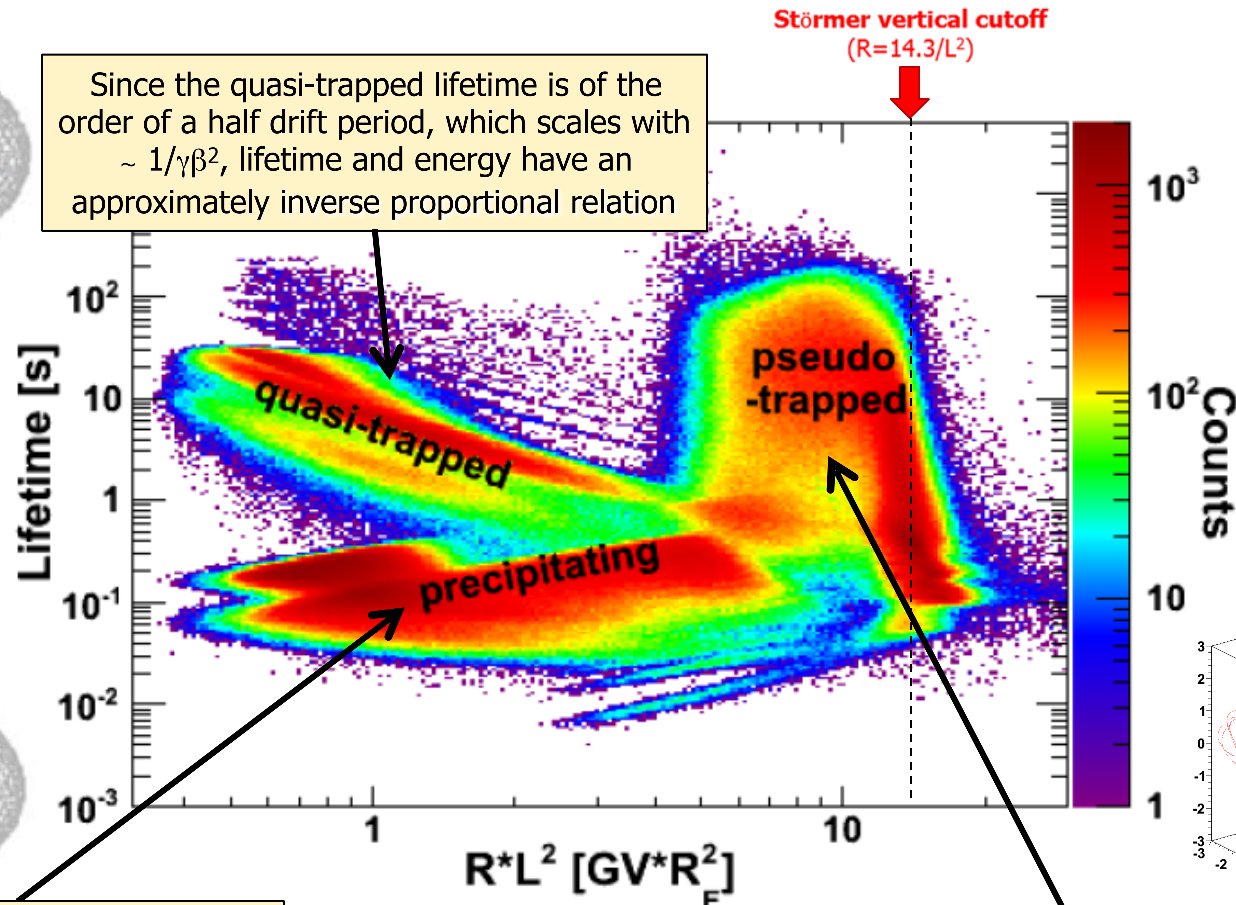

Since the quasi-trapped lifetime is of the order of a half drift period, which scales with ~ $1/\gamma\beta^2$, lifetime and energy have an approximately inverse proportional relation

The precipitating lifetime is shorter than the typical bounce period, which scales with $1/\beta$, resulting in a weaker dependency on energy

Non-adiabatic or large gyro-radius effects cause the breakdown of (quasi) trapping conditions: irregular trajectories with no periodicity

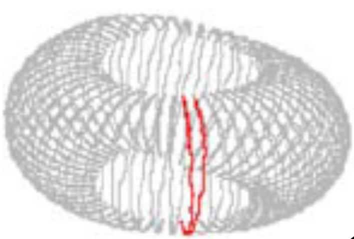

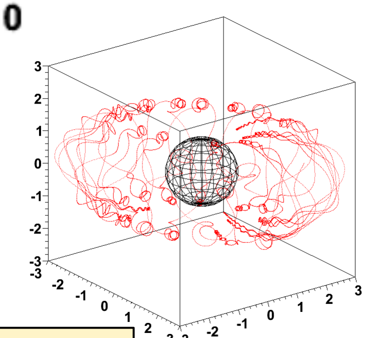

Albedo protons:
origin/impact points

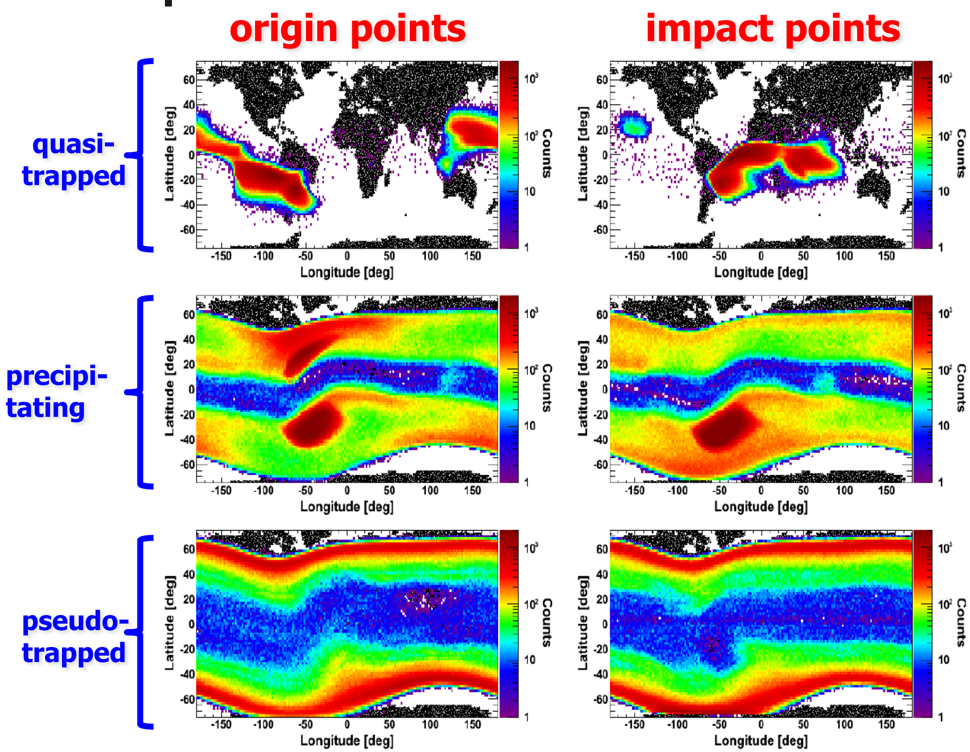

Count distributions of the production (left panels) and absorption (right panels) points on the atmosphere (40 km) as a function of the geographic coordinates.

- **Quasi-trapped**:
  - origin points are located in a region extending westward from the SAA.
  - While drifting from the SAA, protons encounter stronger magnetic fields and the altitude of their mirrors point increases, until they reach again weaker magnetic field regions;
  - then their mirroring altitude decreases and finally they are absorbed by the atmosphere, mainly on the region on the East side of the SAA.
  - Both production and absorption points are located in two regions, in the southern and in the northern magnetic hemisphere respectively, as a consequence of the multipole moment of the Earth's magnetic field.

- **Un-trapped**:
  - **Precipitating:**
    - since they are created and absorbed by the atmosphere in a very short time, their production and absorption points are located near the detection position, populating the whole geomagnetic region explored by PAMELA;
    - indeed, absorption points have a peak in the SAA, while origin points have an additional peak in the northern magnetic region corresponding to southern mirror points in the SAA.
  - **Pseudo-trapped:**
    - Similarly, production and absorption points for such a component spread over all longitudes.

Albedo protons

Flux maps

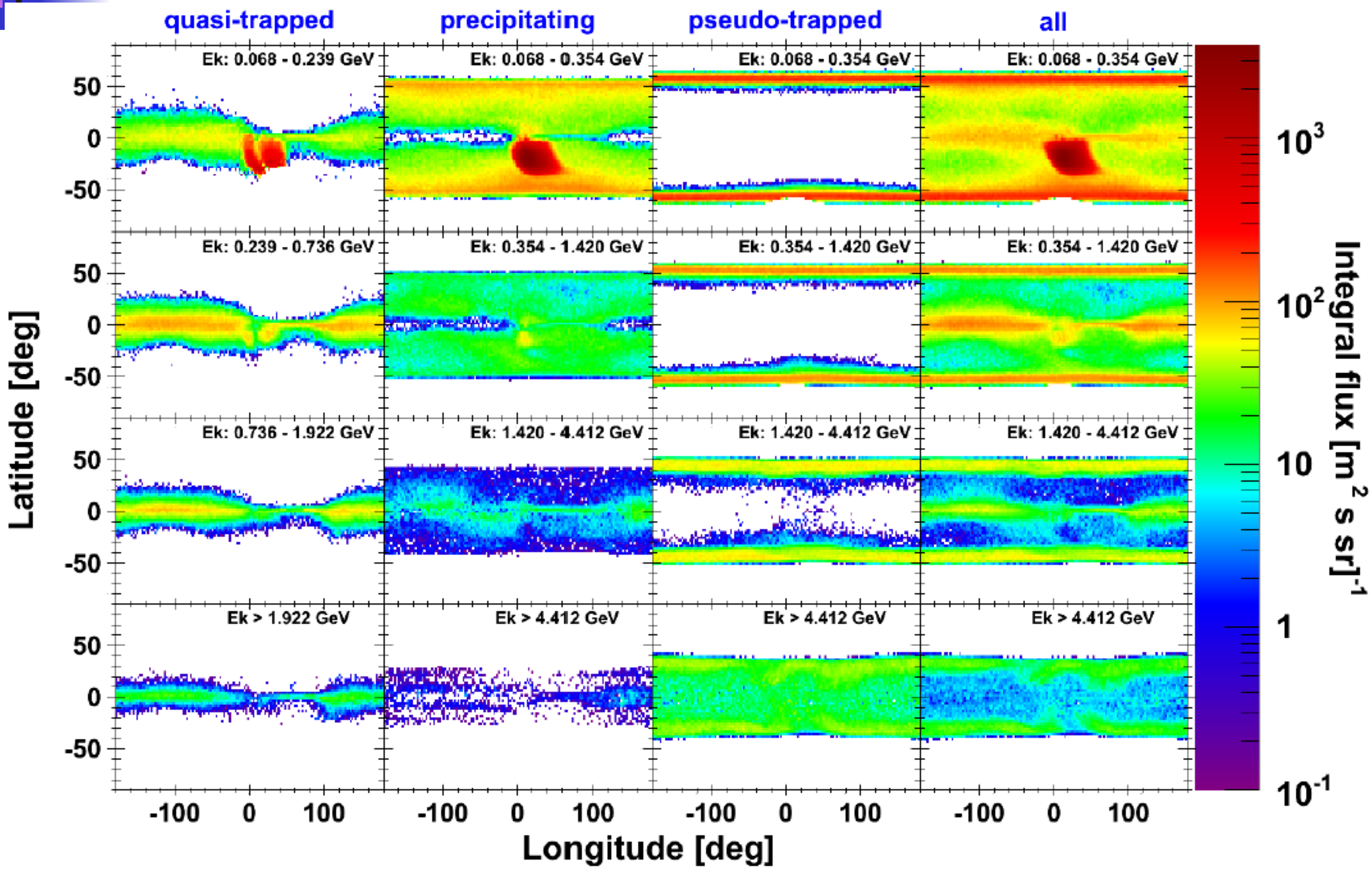

Under-cutoff proton integral fluxes ($m^{-2}s^{-1}sr^{-1}$) as a function of magnetic longitude and latitude, for different energy bins. Results for the several proton populations are reported (from left to right): quasi-trapped, precipitating, un-trapped and the total sample.

Albedo protons

Energy spectra vs latitude

Differential energy spectra outside the SAA region measured for different bins of magnetic latitude (see the labels).

Results for the different proton populations are shown: quasi-trapped (**blue**), precipitating (**green**), pseudo-trapped (**red**) and interplanetary (**black**).

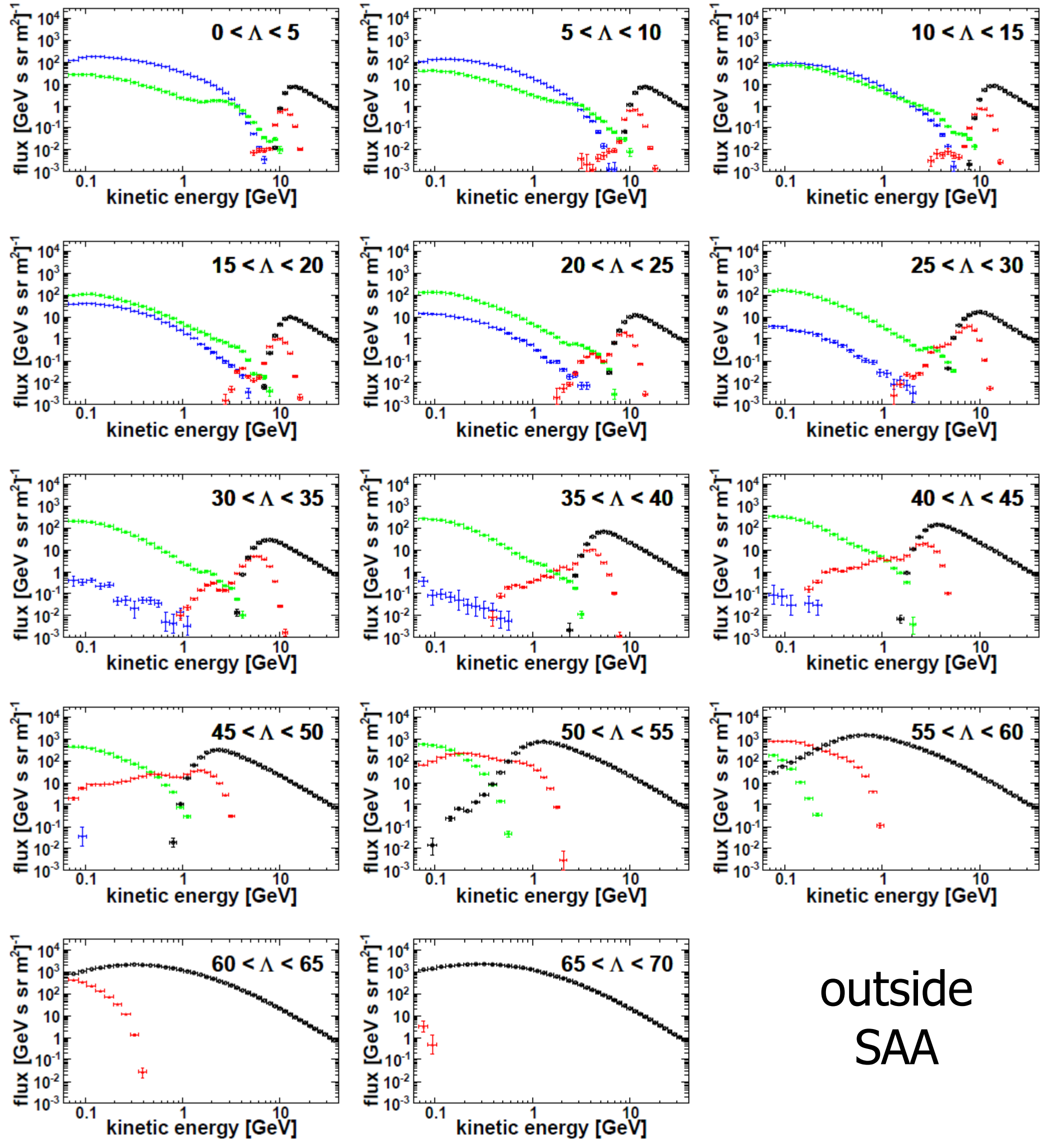

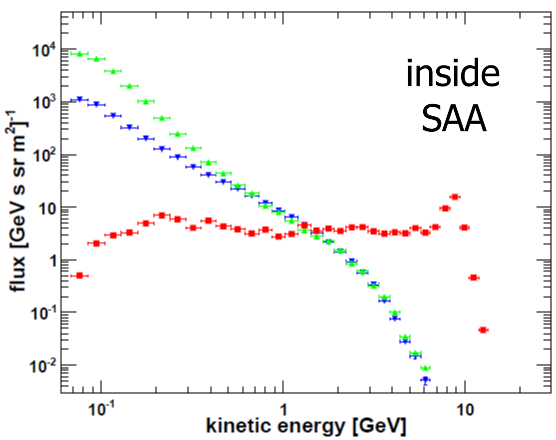

Differential energy spectra in the **SAA** region (B<0.23 G)

Penumbra region

Penumbra: region where protons of both interplanetary and atmospheric origin are present

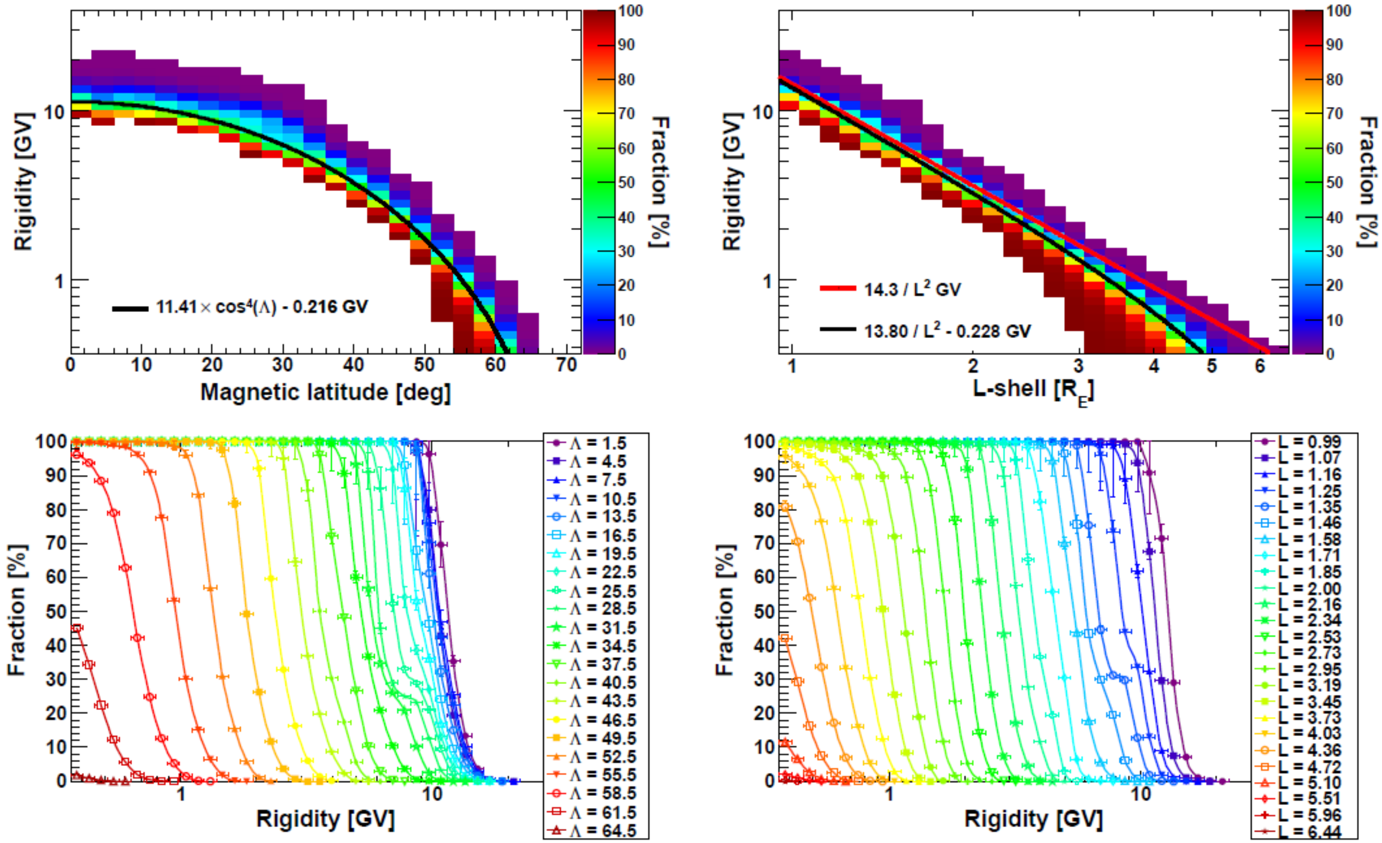

Top panels: fraction of albedo protons in the penumbra region, as a function of particle rigidity and magnetic latitude (left) and McIlwain's L-shell (right); black curves are a fit of points with equal percentages of interplanetary and albedo protons, while the red line denotes the Störmer vertical cutoff for the PAMELA epoch.
Bottom panels: corresponding rigidity profiles, for different values of magnetic latitude (left) and McIlwain's L-shell (right); values at bin center are reported in labels. Lines are to guide the eye.

Geomagnetically trapped antiprotons

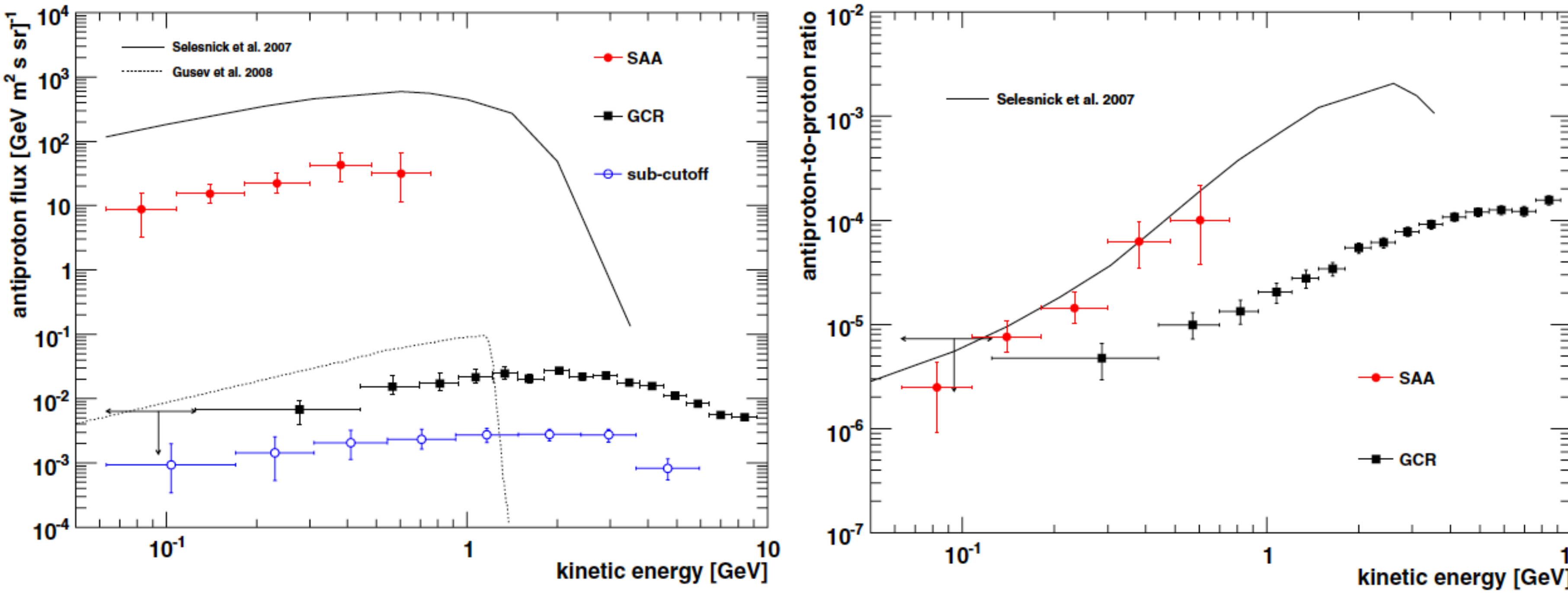

Main source: decay of albedo antineutrons

Geomagnetic cutoff variations

2006 Dec 14 geomagnetic storm

Time profile of the geomagnetic cutoff latitudes measured by PAMELA for different rigidity bins

Data missing from 10:00 UT on Dec 13 until 09:14 UT on Dec 14 because of an onboard system reset of the satellite

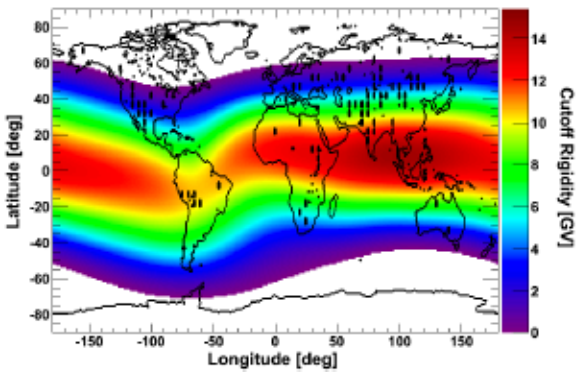

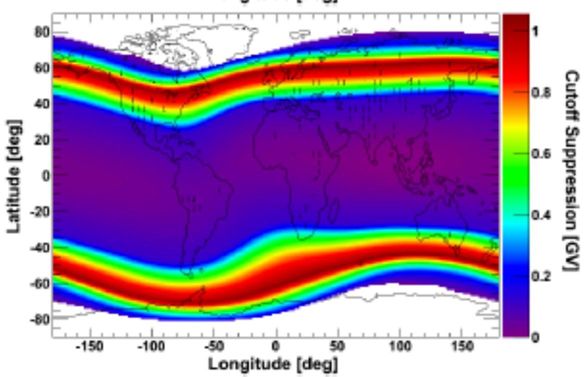

cutoff map at time of maximum suppression

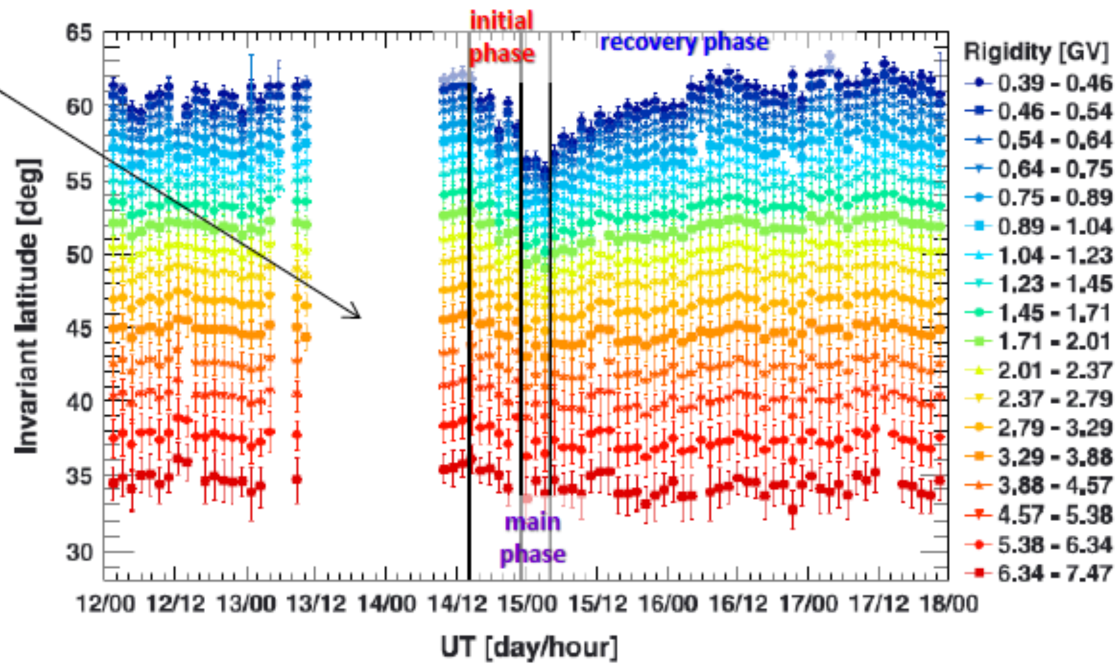

The evolution of the magnetic storm followed the typical scenario in which the cutoff latitudes move equatorward as a consequence of a CME impact on the magnetosphere with an associated transition to southward IMF B_z.

Adriani et al., Space Weather, 14, 2016